Atlas dynamic liner models using Spice

R. G. Watt, 971008

Introduction and circuit description.

Atlas is a large pulsed power experimental facility being designed at the Los Alamos National Laboratory[1]. The 36 MJ capacitor bank will be used for hydrodynamics experiments using imploding metal liners. The liner implosions should reach velocities in the range of 20 km/sec, and should be capable of producing material shocks in an impacted central object in the 10-30 Mbar range. 152 two-stage Marx banks are combined into 38 maintenance units for ease of maintenance. The maintenance units are connected to the central load assembly by oil-filled vertical triplate transmission lines (VTLs) designed to minimize both the transfer inductance and the forces on the lines. Normal operation of the bank should produce current levels in the 40 - 50 MA range in the imploding liner, with current peaking at about 5 μs and liner implosion times in the vicinity of 7-8 μs, dependent on the liner design. The machine design includes an option to switch from the normal 240 kV operating mode to a second operating mode at 480 kV for potential use as a soft x-ray source with about 2 MJ output in the sub-kV x-ray range.

This report summarizes some of the results of Atlas circuit simulations for the VTL based design, using Spice. Two spice models of the machine exist, one with a static liner, and one with an imploding liner. Both models utilize the Ispice4 simulator from Intusoft. Both models approximate the tapered VTL using a 6 segment LC circuit.[2] The VTL model allows estimates of the voltage oscillation due to the inductance and capacitance in the transmission line. The segmented circuit uses a resistor in series with the capacitance of each cell to critically damp each LRC segment. This damping reduces oscillating voltages to realistic levels, while still allowing transient response in the line. The VTL is connected to the final liner load assembly by a simple inductance representing the diskline and power flow channel. The static liner model approximates the load as a simple inductance derived from the physical dimensions of the return conductor and liner outer diameter at time zero. The dynamic liner model incorporates both the implosion pressure response and consequent inductance change upon

---

[1] *An overview of the Atlas Pulsed-Power System*, W. M. Parsons, 11th IEEE International Pulsed Power conference, Baltimore, Md. July 1, 1997.

[2] One should keep in mind the fact that a discrete undamped LC model always produces more severe ringing than an ideal line, and thus presents the worst case estimate. The critically damped version gives an oscillation slightly larger that Gribble's ideal line model. Without critical damping, the segmented model oscillation voltages are larger by 20% than those given by his model. The critically damped version is several kV larger than his 200kV ideal peak.

collapse of the liner. The data of Tucker and Toth [3] are used to follow liner resistivity changes due to heating. The liner implosion is clamped upon reaching a preset final radius (typically of order 5 mm for a 5 cm scale heavy liner). Starting radii, final inner radius, thickness of the liner, length of the liner, and density of the liner are all adjustable. A liner with an outer radius of 5.3 cm and a thickness of 1.86 mm has been used in the calculations shown here, with return current radius at 5.925 cm. The current in the liner can be shunted to ground by a parallel crowbar resistance, if desired. The value of this crowbar must be experimentally determined. The crowbar has the effect of holding liner current up at late time, and has implications for both destruction level in the load assembly and the value of the voltage reversal on the Marx bank capacitors. (Values in the range 10-1000 $\mu\Omega$ seem appropriate based on Pegasus data.)

This set of models is not intended to replace the modeling done by Gribble using the SCAT code, but rather augment it with similar models using different switch characteristics and liner calculation techniques. A comparison of the liner implosion with Gribble's SCAT results, with identical static circuit parameters, shows agreement in current peak to 0.1%, with the implosion time in agreement to within 150 ns. As usual, one must tailor the code inputs to agree with the experimental observations before relying on the results of future simulations for experimental design and extrapolation. The package produces circuit diagrams for self-documentation which are unavailable for SCAT models unless drawn by hand. The models are available upon request for use by anyone having a compatible Spice simulator. The behavioral modeling done for the switches and the imploding liner may provide a difficulty for users with packages written by other vendors.

Model details.

In addition to the VTL, each Atlas model has a simple inductance for the transition section between the transmission line and the diskline that connects to the implosion liner. The net oil VTL inductance used here was 2.785 nH, based on the formula for a 7.7 m long, tapered (from 6' to 2') transmission line with a 1" oil filled triplate gap. The transition section inductance used was 1.54 nH, and essentially accounts for the balance of the Flux3D total inductance calculation for the VTL plus transition section as calculated by Gribble [4]. The net inductance between the output shorting switch in each maintenance unit and the diskline at 26" hot conductor radius for the present engineering design totals 4.32 nH. [5] Both

[3] Tucker and Toth, Sandia Laboratory note SAND-75-0041, April 1975.

[4] *3D Atlas vertical plate oil transmission line field calculations*, R. F. Gribble, LANL internal memo, 9/18/97.

[5] The triplate used in this model is somewhat longer than the current physical design of 6.85 m. The ideal VTL model used in the formula does not properly account for end effects, so

Atlas models are broken into 4 detailed Marx banks and two additional simplified banks representing the balance of the energy storage system.

The detailed Marx circuit contains the storage capacitors and their inductance, the railgaps and their internal inductance and resistance, the series damping resistor, the shunt resistance and inductance, and realistic parasitic elements. The railgaps are broken into a long and short section, with 17 and 8 nH inductance, respectively. This allows injection of the trigger system pulse into the circuit in a realistic manner. The capacitance of the railgap is included, with 10 and 20 pF values in the two sections. The railgap switch model used is a simple exponential drop in switch resistance with an adjustable e-folding time [6], typically set to 2.5 ns. This produces a resistance fall in the switch that bottoms out to a preset 2.4 $\mu\Omega$, in agreement with the value predicted by the Martin model, in 30-40 ns. Each switch can be set to fire at an independently controlled time, as can each half of a particular railgap. (Single channels are modeled by replacing the net 25 nH railgap inductance for normal operation with an 80 nH inductance, partitioned into two parts as in the normal case.) The series damping resistor is 152 mΩ as recently settled on to allow reduced voltage operation within the reversal specification on the capacitors. The shunt resistance and inductance is set to 5 Ω and 70 nH respectively. The fourteen 9' RG-220 output cables are represented by an additional 50 nH in each Marx. The output shorting switch is represented by a 22 nH inductance in each of the four Marx modules that drive a given switch.

The detailed Marx circuit includes the trigger system to realistically estimate the amount of circulating current [7] and ringing voltage in the trigger cables. The trigger circuit uses a switched coaxial storage line as in the real system but only uses a single switch with a single bypass capacitance, rather than the more complicated two gap model used in some recent work by Gribble. Four individual Marx circuits (A1-4) contain a complete single trigger system and module interconnects, railgap stray capacitances, and all major parasitics. This set of 4 Marx modules drives one VTL. The remainder of the circuit consists of two 74

---

differences between the actual VTL and this ideal model must be accounted for in other ways. The transition inductance in the model is used to compensate for differences as the physical design evolves, while keeping the net inductance in agreement with the most recent Flux3D calculations.

[6] This model does not contain the physics of the resistive phase described by Tom Martin, which is used in Gribble's SCAT model. Comparison of the results from these models, the SCAT model, and a simple 2.4 $\mu\Omega$ constant resistance switch model show that the switch characteristics are unimportant in this circuit due to the slow risetime of Atlas, except perhaps in parasitic calculations. The Spice and SCAT simulations are cross checked against each other frequently, to maintain consistency in the circuit assumptions and check the simulation integrity.

[7] Typically there is < 2.5 kA oscillating in each cable. Ringing voltages in normal operation are dominated by the trigger pulse response rather than a response to the Marx erection.

Marx equivalents to drive the final load assembly to the full system level. Constructing various levels of detail allows complete analysis of fault modes in the detailed sections while retaining a small simulation environment for rapid calculation. The separation of the balance of the driver into two 74 Marx equivalents allows an analysis of the effect on the circuit of having half the machine misfire due to a fault or an intentional misfiring to produce a foot on the drive pulse. The major component values are shown in Table 1. The elements shown with a gray background in Table 1 constitute the series inductance in the circuit, with the final entry being the total of those elements exclusive of the liner inductance.

Circuit element	value (as seen in a single Marx, 152 ea.)	single circuit equivalent
Series R	152 mΩ	1.0 mΩ
Capacitance (each)	33 ufd (4 each)	1254 ufd
Capacitor inductance	16 nH (4 each)	0.42 nH
Railgap inductance (MC)	25 nH (2 each)	0.33 nH
Parasitic inductance	108 nH	0.71 nH
Cable inductance	50 nH	0.33 nH
Switch inductance	22 nH	.144 nH
Shunt resistance	5 Ω	33 mΩ
Shunt inductance	70 nH	.46 nH
VTL inductance		2.785 nH
Transition inductance		1.535 nH
Diskline + PFC inductance		4.5 nH
Net VTL + transition		4.32 nH
Net circuit inductance		10.75 nH + Liner
Net circuit resistance		1.05 mΩ
Al Liner OD		10.6 cm
Liner thickness		0.186 cm
Liner height		4.0 cm
Static liner inductance		0.9 nH

Table 1 Circuit parameters.

The circuit diagram is broken into multiple pages as shown in the Appendix. The values used in the detailed Marx, and the associated lumped inductances in the 74 Marx equivalent, are values arrived at in conjunction with Gribble and Cochrane.

The parasitic labeled LVLxx is the return parasitic for the backplane where the series resister and cable header is located. The final load following the VTL model in the circuit is comprised of the 4.5 nH inductance due to the diskline and conical section of the PFC and the 0.9 nH static liner or the imploding liner inductance, depending on the model. The liner resistance (BRLINER) is in series with the liner inductance. The crowbar switch (XCBAR) and its resistance (RCBAR) are in parallel with the liner in the imploding liner model.

Imploding liner model.

The dynamic liner is modeled as a single incompressible shell of predetermined volume. It's trajectory, inductance, and resistance are tracked. The liner motion is calculated as a volume conserving system based on the outer radius position as driven by the liner current induced pressure. Note that such a calculation typically overestimates the velocity of the inner surface as a function of time. This overestimate may be as much as a factor of 2 based on comparisons to material hydrodynamics codes. Consequently, the velocity produced in the model should only be viewed as an indicator of general behavior rather than as a final design parameter. Fortunately, since the major portion of the liner collapse occurs during a small interval near the end, the collapse time is not anywhere near as uncertain as the final velocity may be. The same statement is true of the results of current SCAT calculations. The resistivity of the liner can be followed, looking for an inflection point in it's history which marks that point in time where the resistivity peaks prior to burst. No attempt to account for the plasma following burst was made, so calculations in which melt and burst are seen to occur must be considered to break down at the burst time.[8] The single shell used here does not burst during the calculation. The liner implosion is governed by the acceleration equation

$$d^2r/dt^2 = -\mu_o I^2 Z / 4\pi r M$$

where r is the outer radius of the liner, I is the current, Z is the liner length, and M is the mass of the liner. The liner inductance is calculated using the standard equation for a coaxial cable of return current radius r_a and inner conductor radius r_b, in which the inner radius is allowed to vary in time according to the acceleration equation above. The length and return current radius are assumed fixed at their initial values.

$$L = \mu_o Z \ln(r_a/r_b) / 2\pi$$

[8] Typically, an implosion with an Al liner less than 0.5 mm thick is needed to observe burst prior to the final clamp at 5 mm radius in these calculations. Liners thicker than this, such as the standard 1.85 mm heavy Atlas liner, do not peak in resistivity during a normal implosion in this single skin model. Multiple skin models may be added at a later date.

The liner resistance (which plays a negligible role in the circuit but does matter in terms of melt) is given by

$R = \rho Z/A$

where A is the cross-sectional area of the liner and ρ is the resistivity as a function of specific energy density (ε_m = time integral of RI^2/M) of the Al liner. The resistivity as a function of ε_m is taken from the data of Tucker and Toth.

Creating a simulation using Spice that would permit the above calculation involved utilizing the nonlinear dependent voltage source (termed a B element) in Ispice4. This element provides an inline calculational capability for generating a voltage based on an equation involving voltages and currents elsewhere in a circuit. In this case, the inputs into the acceleration B element were the current in the main circuit and the voltage from another B element that tracked the outer radius. All physical quantities were treated as voltages by the simulator. The acceleration term was followed by two time integrals implemented using the Ispice4 Laplace s domain behavioral model as an integrator. The resultant displacement was fed back into the acceleration calculation along with the initial outer radius, to produce the time history of the radial implosion. The final inner radius was followed in a separate volume conserving calculation. Both inner and outer radii were clamped when the inner radius reached the limiting radius where an impact target might reside. No attempt to follow the internal dynamics of the liner or allow a bounce upon impact was included. The instantaneous outer radius, length, and return current radius was then used to calculate the liner inductance as a function of time, for application in the main circuit. The calculation of the liner resistance was performed using a behavioral model lookup table for the Tucker and Toth ρ vs. ε_m data. (Different materials would be implemented simply by replacing the data set in the lookup table with the appropriate data set.) A separate B element followed ε_m. The resistance was folded into the series liner resistance term in the main circuit, along with the calculated liner inductance. The detailed circuits used for the liner model are shown in the Appendix in sheet 8 of the schematic.

Simulation results at 240 kV operating voltage.

Figure 1 shows the calculated current waveforms in the liner, using a 240 kV charge voltage with the 1 mΩ series resistance, for the static and dynamic liner case. (A calculation using a single skin SCAT model is included for comparison.) The liner used in this simulation is 68 g, with outer radius 5.3 cm, 1.86 mm thick, made of Al (density 2.73 g/cm^3), with return current radius 5.925 and length 4 cm. This liner is essentially the same liner used by Lee[9] for optimization studies for hydrodynamic experiments. This optimization study was done to decide the voltage level of Atlas. Note that this liner and voltage level can not actually be used on Atlas because the voltage reversal on the Marx capacitors is in excess of 30% at 60 kV charge voltage, far outside the design specification of the capacitors. Lower voltage operation will be required due the reversal specification, resulting in lower current drive and delayed implosions.

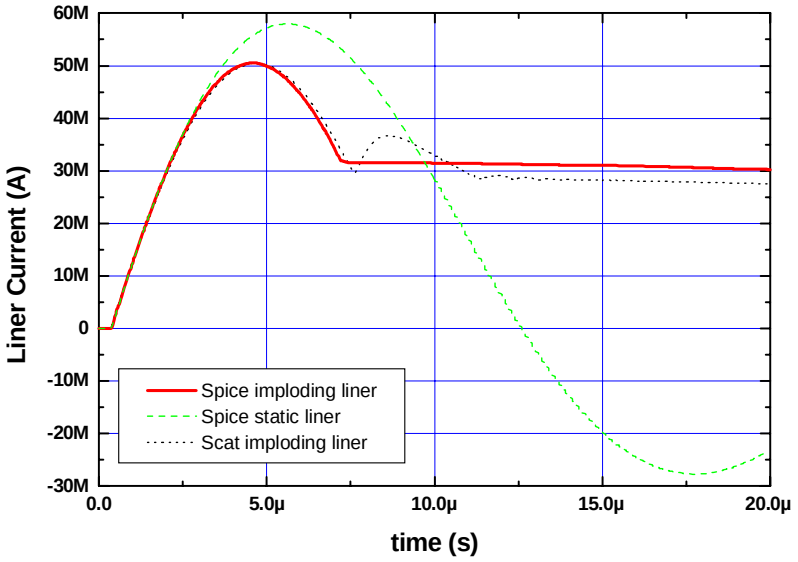

Figure 1. Liner current calculated with a static and dynamic model, at 240 kV and 1 mΩ series resistance.

Figure 2 shows the voltage felt at the liner for the static and dynamic models. Note that the voltage crowbar at 7.5 μs is modeled as a 10 μΩ resistance across the liner, resulting in the voltage dropping to zero at that point. In real experiments, this approximation may not be correct.

[9] Scaling of the optimal hydrodynamic performance in Atlas, H. Lee, internal LANL memo, 3/25/96

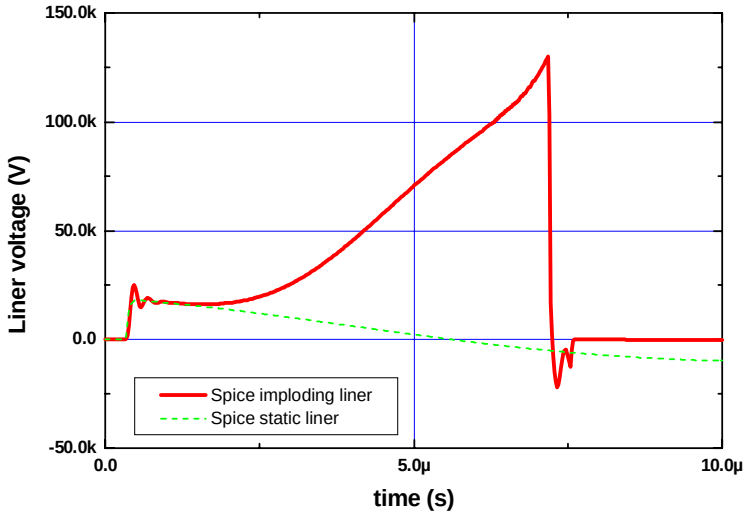

Figure 2. Voltage felt at the liner for the static and dynamic case, at 240 kV charge and 1 mΩ .

Figures 3 and 4 show the liner inductance and resistivity histories in the dynamic model.

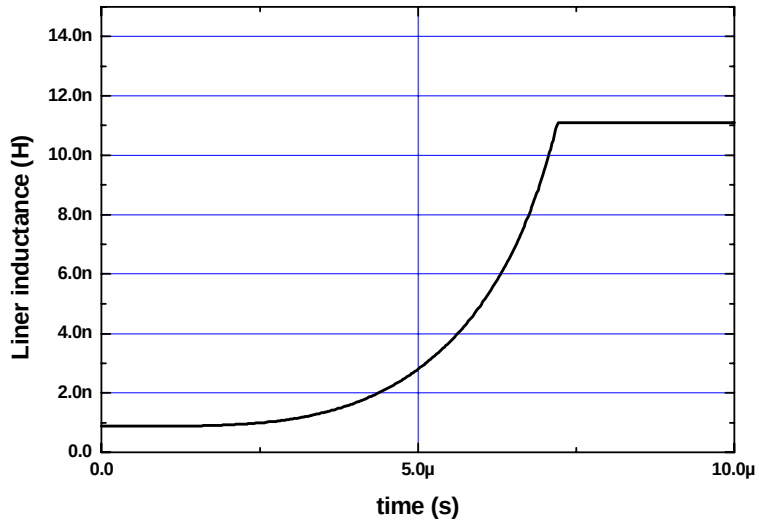

Figure 3. Liner inductance during an implosion at 240 kV charge with 1 mΩ series resistance.

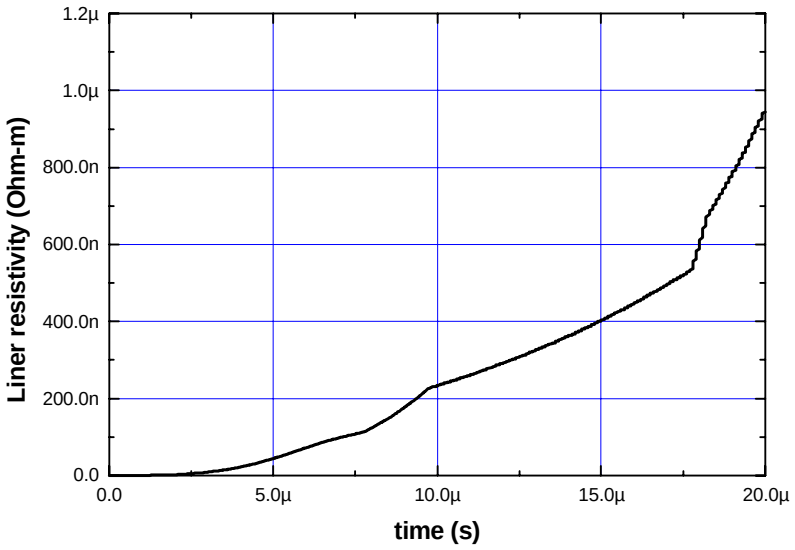

Figure 4. Single skin model liner resistivity, using a 1.86 mm thick liner at 240 kV with 1 mΩ series resistance.

Operation within the voltage reversal specification.

As mentioned above, operation with the present engineering component values and a 240 kV operating level results in a total voltage swing that exceeds the allowed 15% of 60 kV charge on the Marx capacitors. To keep within the voltage swing allowed, one may either increase the series damping resistance at a given charge voltage, at the expense of current drive, or lower both the series resistance and the charge voltage. Cochrane has done a study of this and concluded that an optimal system might use a 50 kV charge and a 1 mΩ series damping resistance[10]. The 1 mΩ series resistance was used in the results discussed above but the charge voltage was held at the original 240 kV level. A series of calculations were later done with the imploding liner Spice model to examine the effects of lowering the charge voltage until, at 50 kV, the total voltage swing was 65 kV, 4 kV less than that allowed. Figure 5 shows the current waveforms, including a 10 mΩ crowbar within several 100 ns of the liner collapse time, for 50, 55, and 60 kV charge voltage on the capacitors. As noted by Cochrane, the 50 kV operating level is safe, but operation above this will require slowly increasing the charge level while observing the operation, to insure that the reversal specification and other operating constraints of the system are not exceeded. Figure 6 shows the voltage appearing across the liner,

[10] *Atlas series resistance*, J. C. Cochrane, LANL internal memo 9/3/97.

and at various locations within the vertical transmission line for 50 kV operation with the 1 mΩ series damping resister.

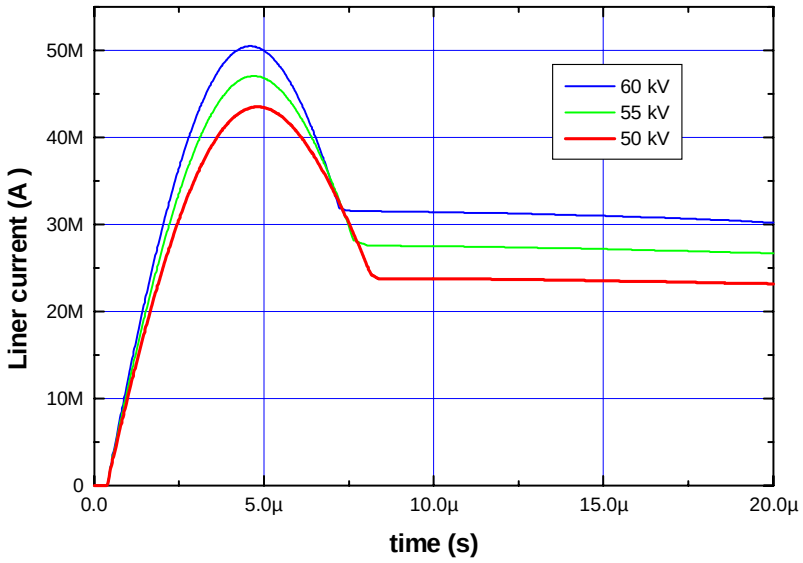

Figure 5. Current waveforms, including crowbar clamping, as a function of charge voltage with 1 mΩ series resistance.

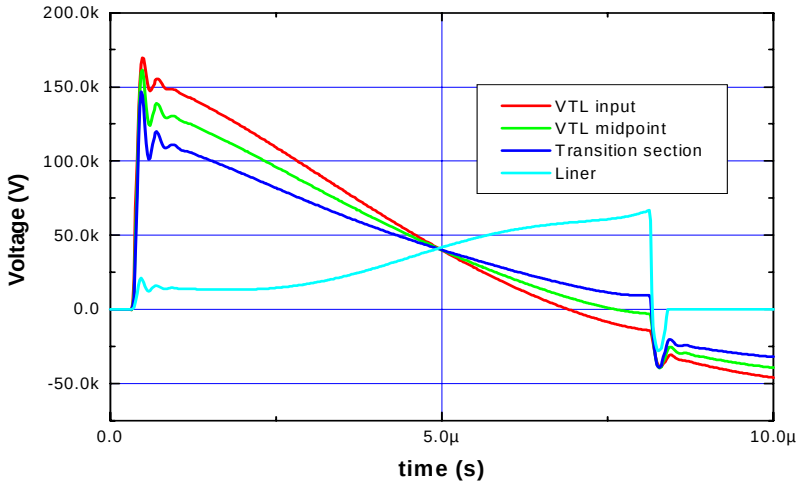

Figure 6. Voltage appearing at various locations in the transmission line system at 50 kV charge.

Figure 7 shows the liner radius as a function of time for this operating voltage with the normal 68 g liner. Finally, Figure 8 shows the liner velocity as a function of time. Remember that this is an over-estimate based on an incompressible liner model. The real velocity is probably less that the calculated by some factor perhaps as large as two.

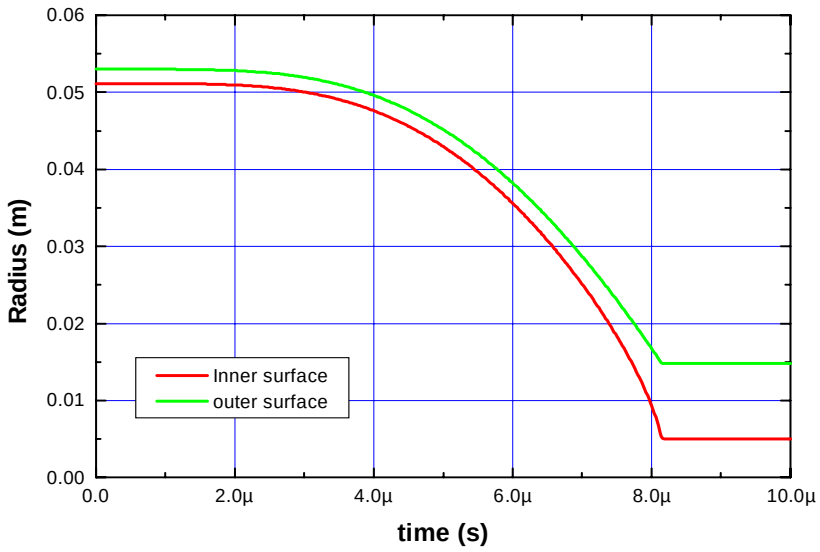

Figure 7. Liner position during a 50 kV charge implosion.

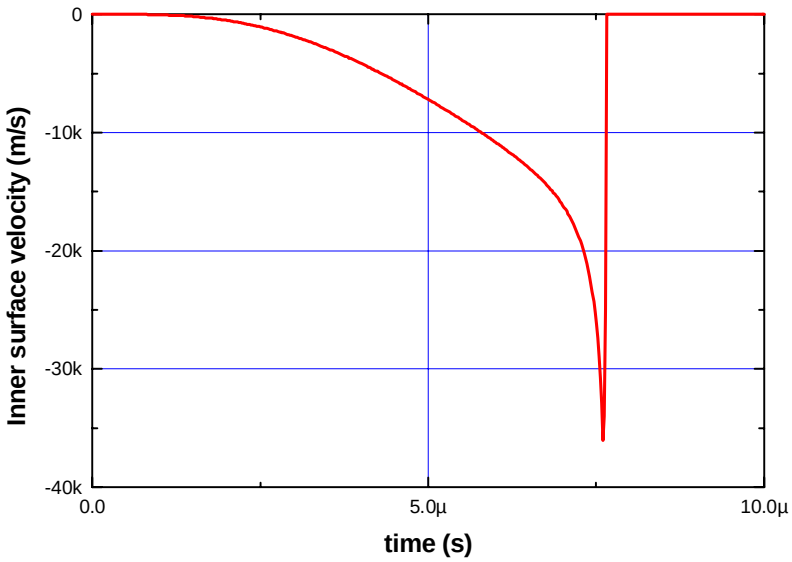

Figure 8. Calculated liner inner surface velocity at 50 kV for a 68 g liner.

Appendix: circuit schematics.

Four of the eight schematic sheets are shown below. Four detailed Marx circuits similar to Marx A1 (sheet 1) are present in the full model. The balance of the driver is shown in sheet 5. Power supplies are shown for all banks to enable correct simulation biasing at time zero in Spice, and to allow one to assess circulating currents in the supply lines. Additionally, the power supply in the trigger circuit is floated to allow accurate evaluation of the shield voltage level during a shot. The reversal diodes in the various Marx charging configurations have been left out of the diagrams, as shown, but when those diodes are placed in the anticipated position, the correct clamping effect is observed. The trigger system is presently constructed as in the prototype Marx, with capacitors on both sides of the trigger cables. The liner implosion calculation is done on sheet 8, using the Spice B element code capability, combined with Laplace integrator blocks. The VTL, power flow channel, and liner assembly are shown on sheet 2.

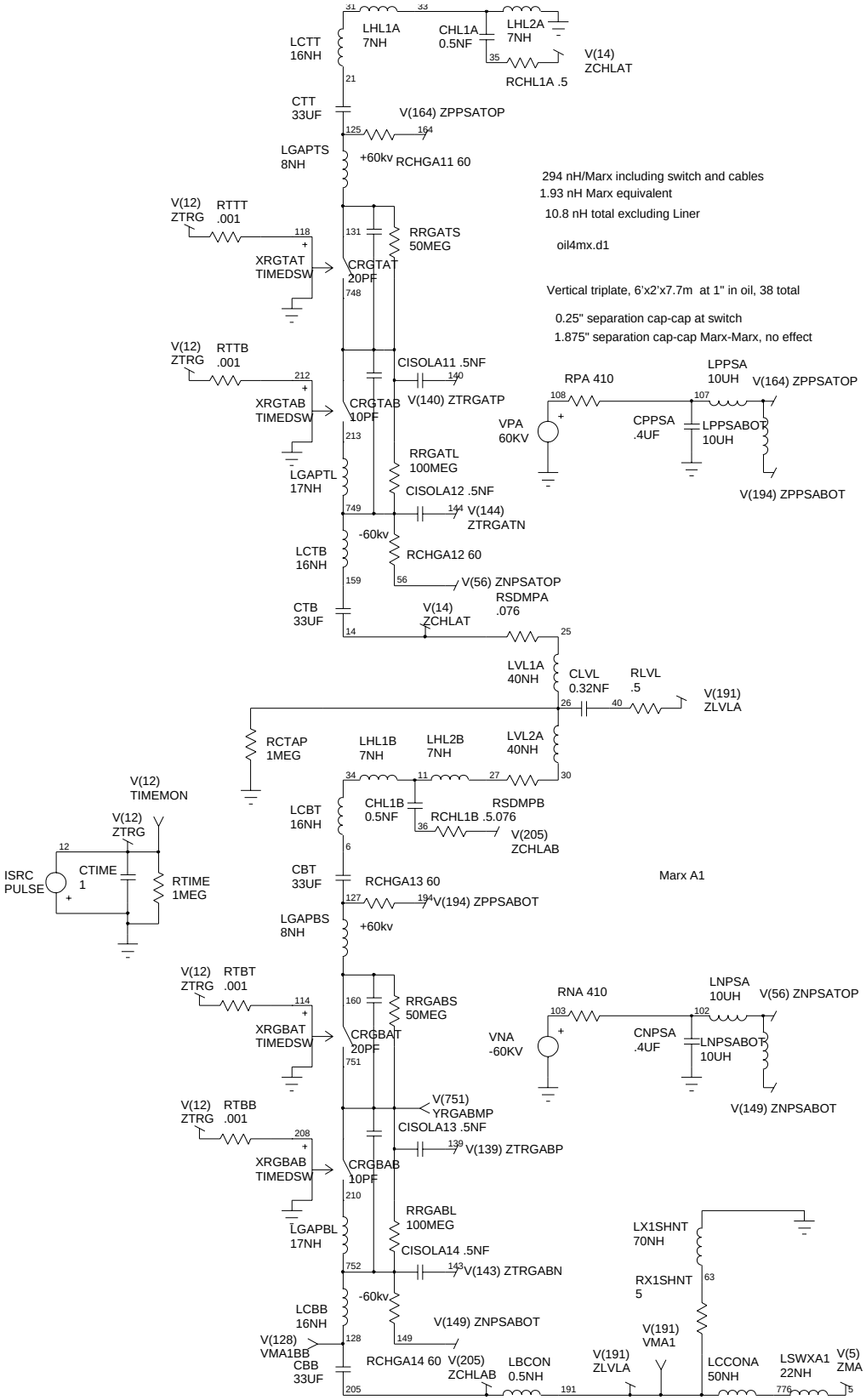

Sheet 1. Detailed Marx module (one of 4 in the model).

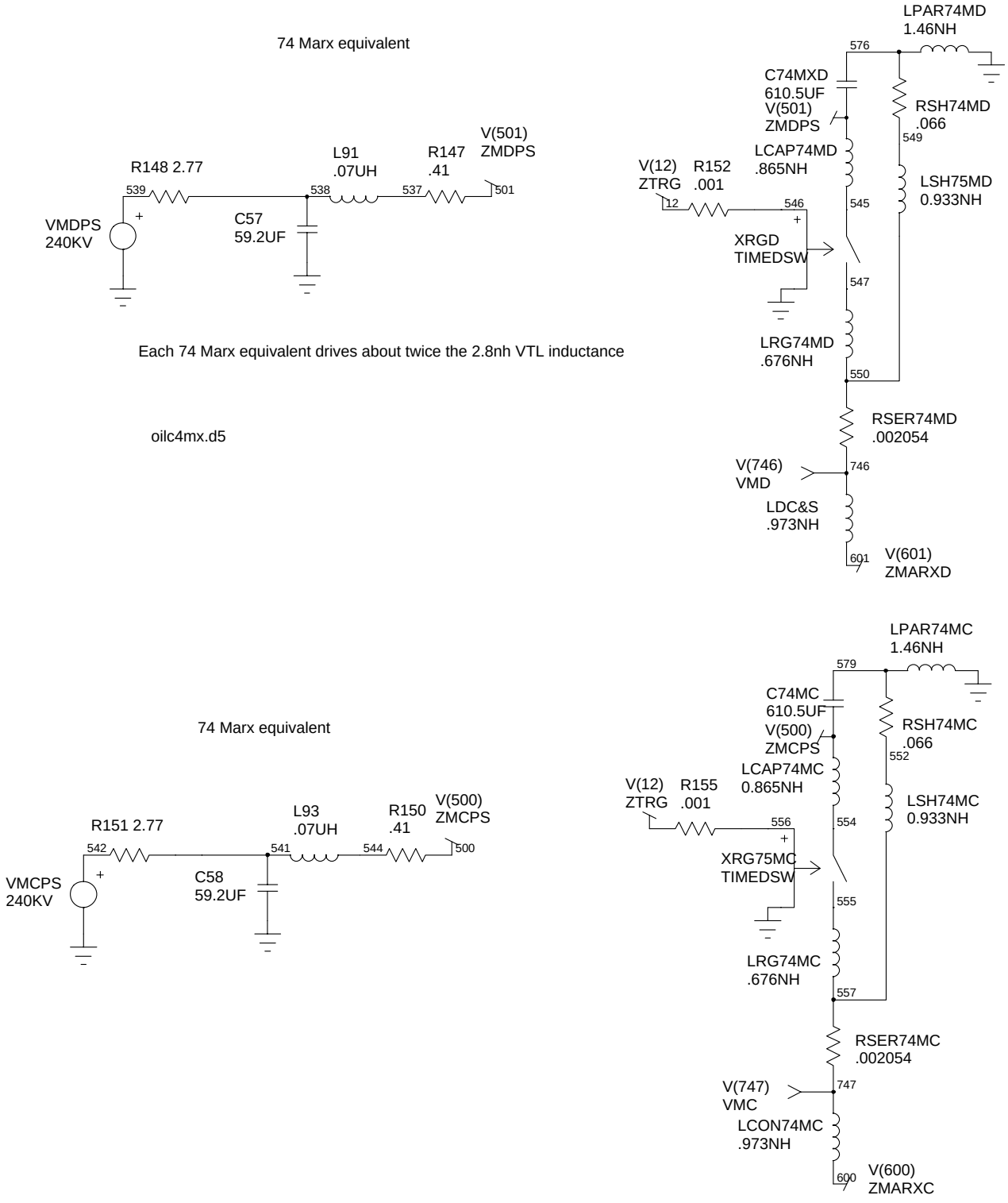

Sheet 5. Balance of Marx circuit (148 Marx modules out of 152 total).

oil VTL modeled at 6 equal length segments, 6’ to 2’, 1 " spacing, 7.7m total

1.54nH transition for 4.32nH total 970926

Total VTL inductance, 2.785nh oil4mx.d2

Liner model is single shell with TT resistivity

VTL loses modeled as critically damped RLC segments

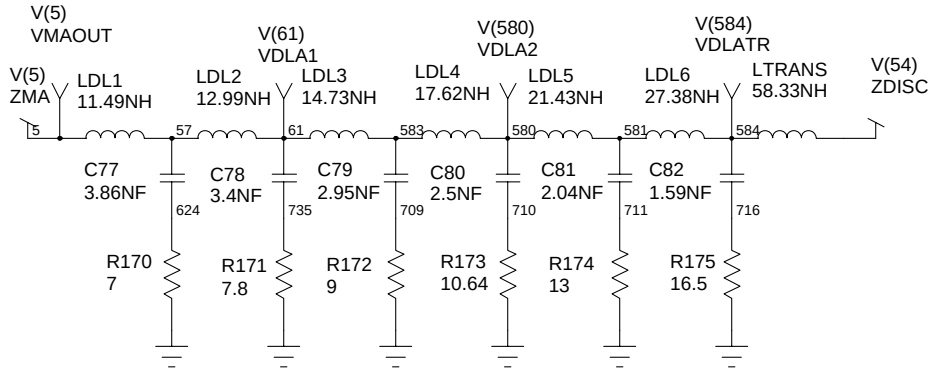

4 individual Marx drive this one VTL

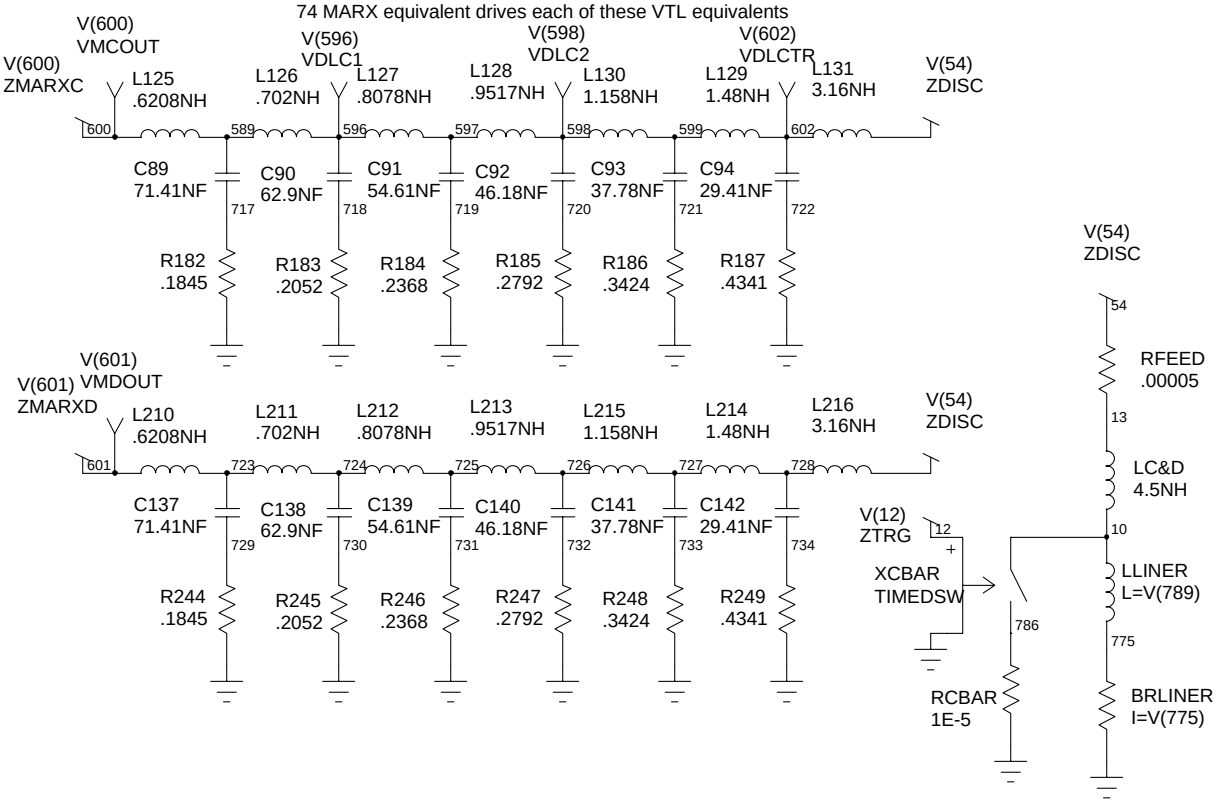

Sheet 2. VTL model, diskline and power flow channel, and liner load assembly.

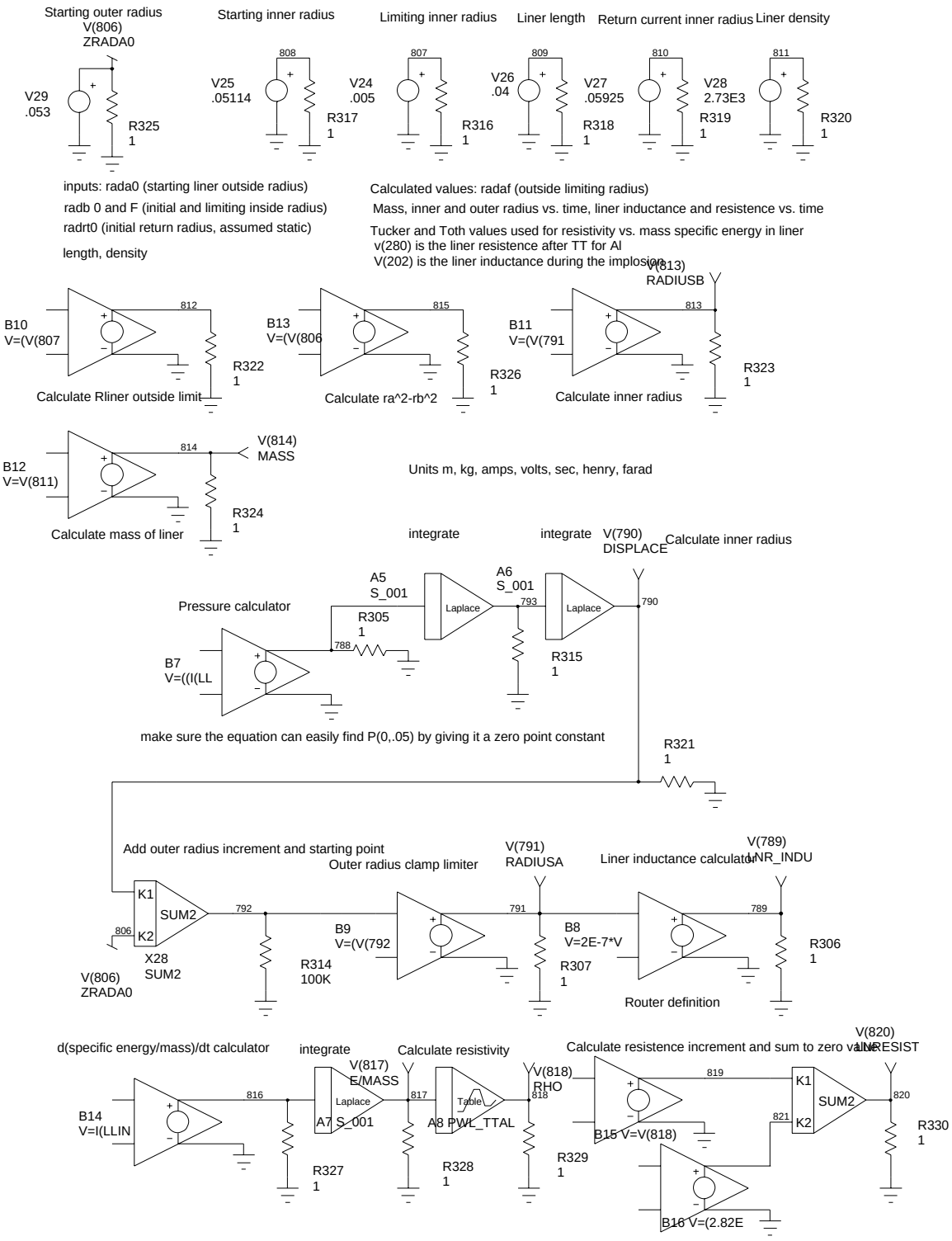

Sheet 8. Dynamic liner model. Inputs are at the top of the schematic.